JACS
JOURNAL OF THE AMERICAN CHEMICAL SOCIETY
Article
Cite This: J. Am. Chem. Soc. 2018, 140, 11370−11377
pubs.acs.org/JACS

Synthesis of Water-Soluble $[Au_{25}(SR)_{18}]^-$ Using a Stoichiometric Amount of $NaBH_4$

Tiankai Chen,[†] Victor Fung,[‡] Qiaofeng Yao,[†] Zhentao Luo,[†] De-en Jiang,[‡] and Jianping Xie*[,†]

[†]Department of Chemical and Biomolecular Engineering, National University of Singapore, 4 Engineering Drive 4, Singapore 117585, Singapore

[‡]Department of Chemistry, University of California, Riverside, California 92521, United States

Supporting Information

ABSTRACT: Determination of the stoichiometry of reactions is a pivotal step for any chemical reactions toward a desirable product, which has been successfully achieved in organic synthesis. Here, we present the first precise determination of the stoichiometry for the reactions toward gold nanoparticle formation in the sodium borohydride reduction method. Leveraging on the real-time mass spectrometry technique, we have determined a precise balanced reaction, $32/x\ [Au(SR)]_x + 8\ e^- = [Au_{25}(SR)_{18}]^- + 7\ [Au(SR)_2]^-$ (here SR denotes a thiolate ligand), toward a *stoichiometric synthesis* of water-soluble $[Au_{25}(SR)_{18}]^-$, where 8 electrons (from reducing agents) are sufficient to react with every 32 Au atoms, leading to the formation of high-purity $[Au_{25}(SR)_{18}]^-$. More interestingly, by real-time monitoring of the growth process of thiolate-protected Au nanoclusters, we have successfully identified an important yet missing byproduct, $[Au(SR)_2]^-$. This study not only provides a new method for Au nanocluster synthesis using only a stoichiometric amount of reducing agent in aqueous solutions (although the synthesis of organic-soluble Au nanoclusters might require a more delicate design of synthetic chemistry) but also promotes the mechanistic understandings of the Au nanocluster growth process.

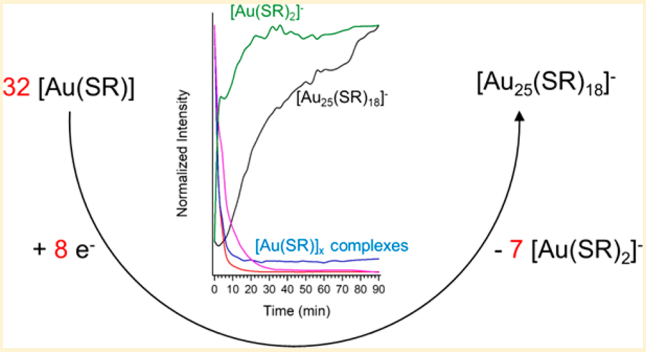

INTRODUCTION

Stoichiometric reactions are the reactions where the reactants are all fully consumed without deficiency or excess after the completion of chemical reactions. Stoichiometric reactions are beneficial, as they are efficient, economic, and environmentally friendly.[1] Ideally, the highest "atom efficiency" of reactions involving multiple reagents can be reached when the reagents are supplied according to the stoichiometry of the reaction. Moreover, supplying a stoichiometric amount of reactant is important in the synthetic chemistry in order to obtain the desired product. For example, either haloalkane or haloalkene can be formed from the halogenation of alkynes depending on the ratio between halogens and alkynes.[2] As a result, the stoichiometric synthesis method is widely applied in both scientific explorations and industrial applications. However, its major application is on organic synthesis, where the stoichiometry of the reactions can be readily determined.[3] To the best of our knowledge, the stoichiometric synthesis on inorganic nanoparticles is limited. For example, in the synthesis of thiolate-protected gold nanoparticles (or thiolated Au NPs for short), one of the most common protocols is the Brust method, where Au(III) salts are first mixed with thiolate ligands to form Au(I)-thiolate complexes.[4] In the subsequent step, a reducing agent, sodium borohydride ($NaBH_4$), is added to reduce Au(I) to Au(0) for the formation of Au NPs. A typically used molar ratio between $NaBH_4$ and Au is 10:1.[5] Under this ratio, the electrons (e^-) received per Au atom are 80, as one $NaBH_4$ molecule is capable of providing 8 electrons in reduction reactions.[6] However, only 1 e^- is required per Au atom for the reduction even if we assume the complete reduction of Au(I) to Au(0), indicating $NaBH_4$ is in great excess (e.g., 80 times higher than the required amount) under this synthesis condition. Nevertheless, whether $NaBH_4$ must be in excess for Au NP formation, or in other words whether Au NPs can be formed by using only a stoichiometric amount of $NaBH_4$, is not known.

Before we could supply the reactants in stoichiometric amount, we need to know the stoichiometry of the reaction. The calculation on the stoichiometry of the $NaBH_4$ reduction reaction of Au NP synthesis can be facilitated by knowing the precise molecular formula of Au NPs. A special class of ultrasmall Au NPs, thiolate-protected gold nanoclusters (or thiolated Au NCs for short), feature a precise molecular formula (and structure), which meets the requirement and can be used as a model system for the investigation.[7] These Au NCs usually contain several to a hundred gold atoms in the core, which is protected by a shell of thiolate ligands. As a

Received: June 13, 2018
Published: August 20, 2018

DOI: 10.1021/jacs.8b05689
J. Am. Chem. Soc. 2018, 140, 11370−11377

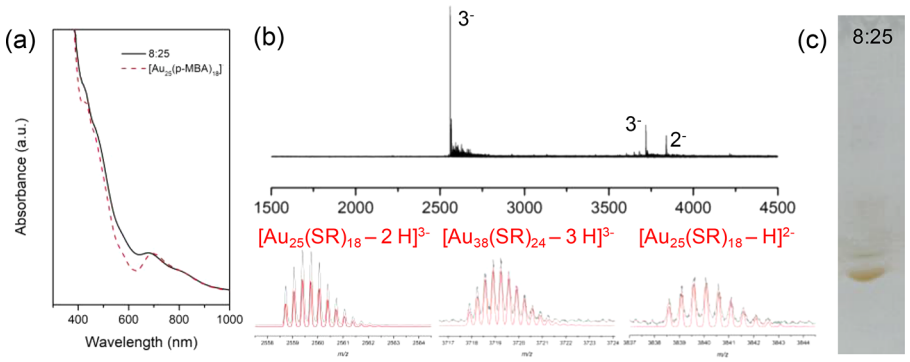

Figure 1. (a, black line) UV–vis absorption, (b, top panel) ESI mass spectra, and (c) PAGE analysis of Au NCs synthesized at $R_{e/Au}$ = 8:25. The red dashed line in (a) is the UV–vis absorption spectrum of $[Au_{25}(SR)_{18}]^-$ prepared via a reported protocol.[10] The bottom panel in (b) is a comparison of experimental (black lines) and simulated (red lines) isotope patterns.

result, the Au NCs can be written as $[Au_n(SR)_m]^q$, where n, m, and q represent the number of gold atoms, thiolate ligands, and the net charge of the Au NCs, respectively. The valence state of Au can be either +1 or 0 in the structure of Au NCs, while the valence state of thiolate ligands is −1.[8] As a result, the number of Au(0) atoms, also known as valence electron count (n^*), can be calculated from the equation $n^* = n - m - q$.[9] For example, n^* for $[Au_{25}(SR)_{18}]^-$ is 25 − 18 − (−1) = 8. This number is also equivalent to the number of e^- required to reduce Au(I)-thiolate complexes to form the target Au NCs. In one of the previous experimental studies on the synthesis of $[Au_{25}(SR)_{18}]^-$ using carbon monoxide (CO), a stoichiometric amount of CO_3^{2-} (corresponding to n^*) was formed.[10] Therefore, the half-reaction of $[Au_{25}(SR)_{18}]^-$ formation from Au(I)-thiolate complexes can be written as

$$25/x\ [AuSR]_x + 8\ e^- = [Au_{25}(SR)_{18}]^- + 7\ SR^- \quad (1)$$

where $[AuSR]_x$ represents a general formula of the reacting oligomeric Au(I)-thiolate complexes. From eq 1, the stoichiometric molar ratio between the e^- provided by reducing agent and Au(I)-thiolate complexes (per Au atoms count) is 8:25 ($R_{e/Au,stoich}$ = 8:25). Hence, the stoichiometry can be calculated for the synthesis of $[Au_{25}(SR)_{18}]^-$, which is 1 mol $NaBH_4$ to 25 mol Au (atoms), as one $NaBH_4$ could provide 8 e^- in the reduction.

Herein, we present the investigation on the synthesis of Au NCs using a stoichiometric amount of $NaBH_4$. Compared with conventional synthesis, the amount of $NaBH_4$ is greatly reduced to the stoichiometric level. However, instead of obtaining pure $[Au_{25}(SR)_{18}]^-$ in the trial, Au NCs with larger n^* also exist in the product. We then try to understand the reaction process by monitoring the changes of intermediate species during the reaction. Surprisingly, we identify an important yet missing byproduct of the reaction, which is $[Au(SR)_2]^-$, instead of free thiolates as previously assumed in eq 1. With this piece of important information, we are able to rewrite the balanced reaction for $[Au_{25}(SR)_{18}]^-$ synthesis, recalculate the stoichiometry ($R_{e/Au,stoich}$ = 8:32), and successfully synthesize monodispersed $[Au_{25}(SR)_{18}]^-$ by only providing the stoichiometric amount of e^- from the reducing agent in solution.

RESULTS AND DISCUSSION

Synthesis of Au NCs with $R_{e/Au}$ = 8:25. The stoichiometric synthesis of Au NCs was based on a modified Brust method,[11] by reducing the amount of $NaBH_4$ according to the stoichiometry in eq 1 (see Experimental Section for details). We chose 4-mercaptobenzoic acid (*p*-MBA) as model ligand and first set the molar ratio between the electrons provided by $NaBH_4$ and Au ($R_{e/Au}$) as 8:25, which is equivalent to the $R_{e/Au,stoich}$ calculated from eq 1. In a typical synthesis, aqueous solutions of *p*-MBA (50 mM, 0.2 mL) and $HAuCl_4$ (20 mM, 0.25 mL) were added to 4.35 mL of ultrapure water (bubbled with nitrogen for 2 min prior to the experiment to avoid oxidation of $NaBH_4$ by dissolved oxygen[12]) under 500 rpm stirring at room temperature. After 30 min, Au(I)-thiolate complexes were formed and 1 M NaOH solution was added to bring the pH of the reaction solution to 11.5. Figure S1 (Supporting Information) shows the mass spectra of the Au(I)-thiolate complexes characterized by electrospray ionization mass spectrometry (ESI-MS). It can be seen that all the peaks in the ESI mass spectrum correspond to Au(I)-thiolate complexes, confirming our hypothesis that Au is in +1 oxidation states prior to $NaBH_4$ reduction. It should be noted that the stoichiometry of this reaction is difficult to calculate because the thiols are in complex oxidation states after this reaction. After that, these Au(I)-thiolate complexes will be reduced by a stoichiometric amount of $NaBH_4$ by adding 0.2 mL of 1 mM $NaBH_4$ solution to the reaction solution under a nitrogen atmosphere. The Au NC product was collected and purified after a 90 min reaction.

Figure 1 shows the UV–vis absorption spectra, ESI mass spectra, and polyacrylamide gel electrophoresis (PAGE) analysis of the as-synthesized Au NCs under $R_{e/Au}$ = 8:25. Figure 1a (black line) shows its UV–vis absorption spectrum. It can be seen that the characteristic peaks of $[Au_{25}(SR)_{18}]^-$ at 430 and 690 nm exist in the spectrum, indicating the presence of $[Au_{25}(SR)_{18}]^-$.[13] However, compared with the absorption spectrum of a pure $[Au_{25}(SR)_{18}]^-$ sample (red dashed line) prepared following a reported protocol,[10] the spectrum is less featured and the absorbance difference between 690 and 630 nm is much smaller. These data suggest that besides $[Au_{25}(SR)_{18}]^-$, other Au NC species also exist in the product. This postulation was further confirmed by the ESI mass spectrum (Figure 1b) and PAGE analysis (Figure 1c). Three sets of peaks can be found in the ESI mass spectrum of the Au NCs. In addition to the two sets of peaks at m/z around 2559 and 3839 (corresponding to $[Au_{25}(SR)_{18}]^-$), another set of peaks at m/z around 3718 exist in the spectrum. The isotope pattern analysis (the bottom panel) suggests that this set of peaks correspond to $Au_{38}(SR)_{24}$. It is consistent with the PAGE analysis, where an additional band with lower mobility

DOI: 10.1021/jacs.8b05689
J. Am. Chem. Soc. 2018, 140, 11370–11377

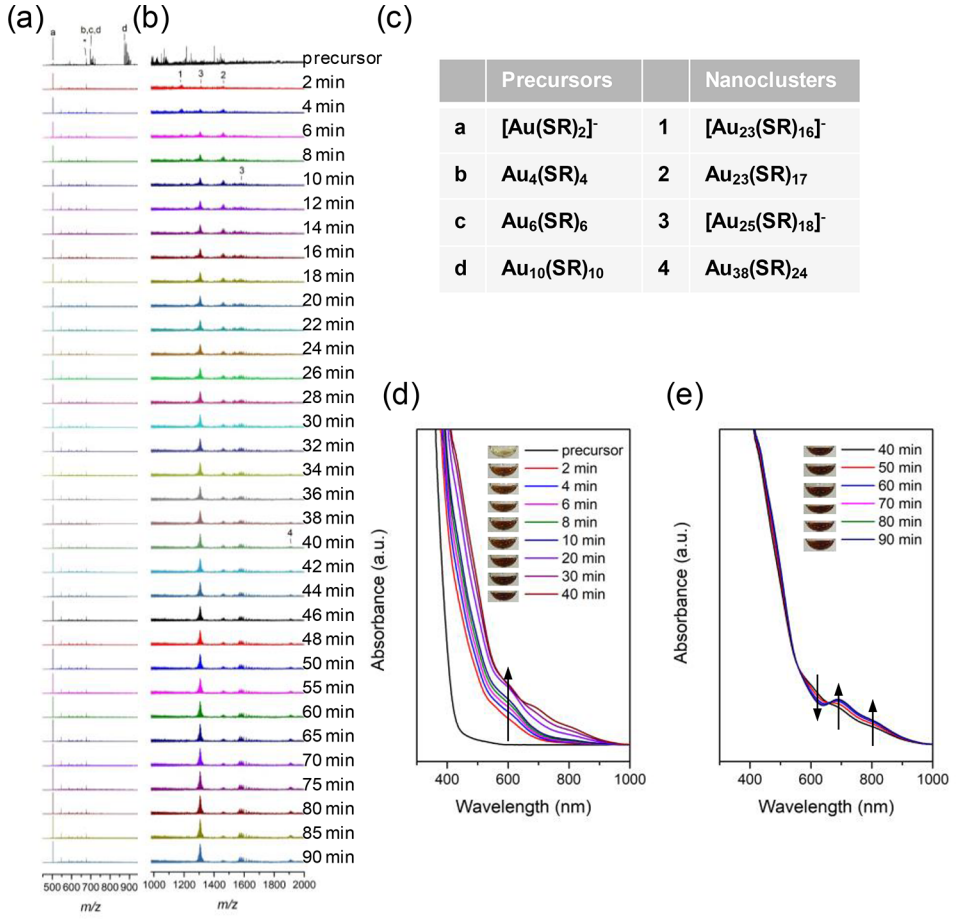

	Precursors		Nanoclusters
a	$[Au(SR)_2]^-$	1	$[Au_{23}(SR)_{16}]^-$
b	$Au_4(SR)_4$	2	$Au_{23}(SR)_{17}$
c	$Au_6(SR)_6$	3	$[Au_{25}(SR)_{18}]^-$
d	$Au_{10}(SR)_{10}$	4	$Au_{38}(SR)_{24}$

Figure 2. Time-evolution ESI mass spectra (from precursors to the reaction mixture at 90 min after $NaBH_4$ addition) of (a) Au(I)-thiolate complexes and (b) Au NC species in the synthesis of Au NCs using $R_{e/Au}$ = 8:25. (c) Formula of the identified Au(I)-thiolate complexes and Au NC species from ESI mass spectra (SR denotes *p*-MBA). (d, e) Time-evolution UV−vis absorption spectra (from precursors to the reaction mixture at 90 min after $NaBH_4$ addition) of the reaction solution with digital photos (inset).

(therefore larger size) exists together with the reddish-brown band for $[Au_{25}(SR)_{18}]^-$. Additionally, the yield of Au NCs was determined to be 79 ± 2% (on a Au atoms basis) by inductively coupled plasma optical emission spectroscopy (ICP-OES).

The existence of $Au_{38}(SR)_{24}$ in the Au NCs synthesized at $R_{e/Au}$ = 8:25 is unexpected, as n^* for this species is 14, which is larger than that of $[Au_{25}(SR)_{18}]^-$. Given that the formation of one $Au_{38}(SR)_{24}$ molecule requires 14 e^- ($R_{e/Au,stoich}$ = 14:38 > 8:25), more electrons are required for the formation of $Au_{38}(SR)_{24}$ from Au(I)-thiolate complexes compared with $[Au_{25}(SR)_{18}]^-$. However, since the number of electrons we provided was the stoichiometric amount for $[Au_{25}(SR)_{18}]^-$ formation, there were no excess electrons for further reduction. Furthermore, as the reaction was carried out in aqueous solution under a nitrogen atmosphere, there were no other reducing agents in solution that could provide electrons to reduce Au(I)-thiolate complexes. Considering the yield of Au NCs was only 79 ± 2%, the possible reason could be that not all Au(I)-thiolate complexes have been reduced and incorporated into Au NCs, leaving excess electrons in solution, which could be utilized to form larger sized $Au_{38}(SR)_{24}$. As a result, although we have successfully demonstrated that Au NCs can be synthesized under low $R_{e/Au}$ ratios (the amount of $NaBH_4$ was reduced by ∼250 times compared with the one used in the conventional synthesis), there were still excess reactants, and hence the synthesis cannot be considered a stoichiometric synthesis.

Discovery of $[Au(SR)_2]^-$ as Byproduct. In order to investigate the reason that part of the Au(I)-thiolate complexes was not reduced and incorporated into Au NCs, we tried to monitor the reduction process of Au(I)-thiolate complexes ($R_{e/Au}$ = 8:25) in solution. Figure 2a and b show the ESI mass spectra of the reaction solution at different times after $NaBH_4$ addition. As the amount of $NaBH_4$ was greatly reduced, the species in reaction solution could be directly characterized by ESI-MS without sample pretreatment (real-time ESI-MS).[14] The experimental peaks were identified and matched with the simulated isotope patterns (Figures S2−S5, Supporting Information), with the formula of the Au(I)-thiolate complexes and Au NC species listed in Figure 2c. For clarity in checking the evolution of the intermediates, the time-evolution peak intensity of these identified species was plotted in Figure 3. Figure 2a presents the evolution of Au(I)-thiolate complexes during the reaction process. It can be seen from this figure and Figure 3 that the intensity of most Au(I)-thiolate complexes (namely, species b to d) decreased quickly after the addition of $NaBH_4$. This is expected, as the Au(I)-thiolate complexes are the reactants for the formation of Au NCs. However, to our surprise, the intensity of species a, $[Au(SR)_2]^-$, increased with the reaction, instead of decreasing in intensity from the reduction reaction. Such substantial increase in intensity

DOI: 10.1021/jacs.8b05689
J. Am. Chem. Soc. 2018, 140, 11370−11377

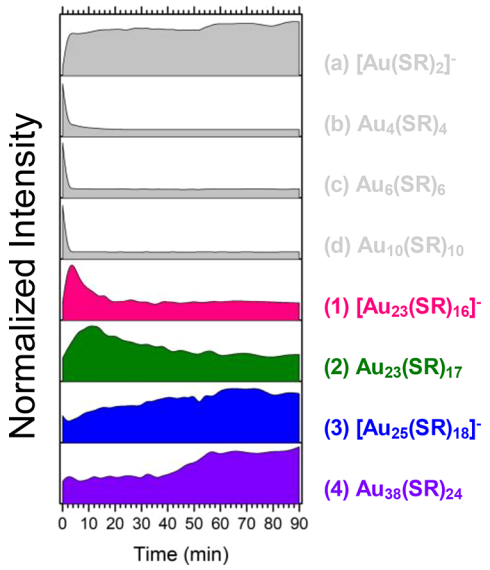

Figure 3. Time-dependent ESI-MS spectral intensity of Au(I)-thiolate complexes and Au NC species in the synthesis of Au NCs using $R_{e/Au}$ = 8:25.

implies $[Au(SR)_2]^-$ as a product formed instead of a reactant being consumed during the reaction. Despite the evolution of Au(I)-thiolate complexes, the evolution of Au NC intermediates can also be monitored, as shown in Figure 2b. The intermediate species that were abundant enough in the reaction solution can be captured by ESI-MS, where species 1 ($[Au_{23}(SR)_{16}]^-$) and species 2 ($Au_{23}(SR)_{27}$) are two important intermediates for the formation of $[Au_{25}(SR)_{18}]^-$ and $Au_{38}(SR)_{24}$.[15] It can be evidenced from Figure 3 that the intermediates were formed first in the reaction but later consumed, converting into species 3 ($[Au_{25}(SR)_{18}]^-$) and species 4 ($Au_{38}(SR)_{24}$), the thermodynamically stable species, in the product. The formation of a mixture of Au NC species, followed by a size-focusing process, is similar to the reported two-step growth mechanism of Au NCs.[10,16] Time-evolution UV–vis absorption spectra of the reaction solution also confirm the two-step mechanism, where there was an increase in absorbance between 400 and 900 nm at the first stage (Figure 2d) and an obvious increase of the characteristic peaks of $[Au_{25}(SR)_{18}]^-$ (Figure 2e) at the second stage.

From the results above, we found that the signal intensity of $[Au(SR)_2]^-$ in the ESI mass spectra increased monotonically during the synthesis, and when the reaction was considered complete after 90 min of $NaBH_4$ addition, the peak intensity of $[Au(SR)_2]^-$ was greatly increased compared with that in the precursors (before the reduction reaction), which suggests that this species ($[Au(SR)_2]^-$) is likely a byproduct of the reaction. To the best of our knowledge, this is the first report on the formation of $[Au(SR)_2]^-$ during the formation of thiolated Au NCs from Au(I)-thiolate complexes, as free thiolates are usually considered as the byproduct in the reported studies.[17] However, we did not detect any free thiolate ligands in the ESI mass spectra, although free thiolates could be captured by ESI-MS under the same ESI-MS operating parameters (Figure S6, Supporting Information). In addition, we found $[Au(SR)_2]^-$ has low reactivity at various reduction environments. We have extracted the Au(I)-thiolate complexes presented in the solution after synthesis using ultrafiltration and tried to reduce them. The corresponding ESI mass spectrum in Figure S7a (Supporting Information) shows that the extracted species were $[Au(SR)_2]^-$ (with an unidentified species *) in the solution. After the addition of 100 mM $NaBH_4$ solution, $[Au(SR)_2]^-$ has been hardly reduced, as negligible changes in the UV–vis absorption spectra were observed (Figure S7b, Supporting Information). Therefore, in the Au NC synthesis process, $[Au(SR)_2]^-$ would survive as a stable byproduct even in the presence of reducing agent in solution. Based on this new understanding, the balanced half-reaction of the reduction from Au(I)-thiolate complexes into $[Au_{25}(SR)_{18}]^-$ can be modified as eq 2:

$$32/x\ [Au(SR)]_x + 8\ e^- = [Au_{25}(SR)_{18}]^- + 7\ [Au(SR)_2]^- \quad (2)$$

Stoichiometric Synthesis of $[Au_{25}(SR)_{18}]^-$. According to eq 2, the stoichiometric ratio $R_{e/Au,stoich}$ is reduced from 8:25 to 8:32, because the byproduct $[Au(SR)_2]^-$ was not reduced or incorporated into $[Au_{25}(SR)_{18}]^-$ as we assumed previously. To further test this postulation, different $R_{e/Au}$ ratios (4:25, 8:32, and 14:38) were used to synthesize Au NCs ($R_{e/Au}$ = 8:32 is the postulated stoichiometric synthesis according to eq 2). The UV–vis absorption spectra of the as-synthesized Au NCs (Figure 4a) indicate that the Au NCs synthesized using $R_{e/Au}$ = 8:32 (red line) have the best defined characteristic peaks of $[Au_{25}(SR)_{18}]^-$ at 430 and 690 nm among the products of the three $R_{e/Au}$ ratios, suggesting its highest monodispersity and chemical purity. The composition of the Au NCs at different $R_{e/Au}$ ratios was further determined by ESI-MS, as shown in Figure 4b. The Au NCs synthesized at $R_{e/Au}$ = 8:32 also show the highest monodispersity, where only two sets of peaks at m/z = 2559 and 3839 corresponding to $[Au_{25}(SR)_{18}]^-$ carrying

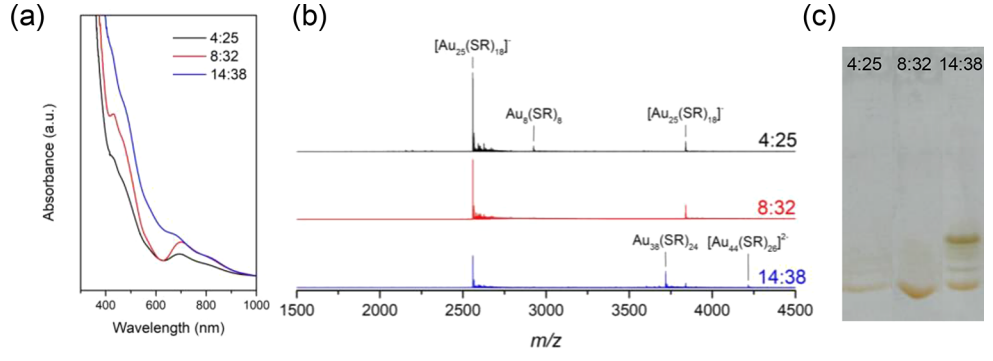

Figure 4. (a) UV–vis absorption, (b) ESI mass spectra, and (c) PAGE analysis of Au NCs synthesized under different $R_{e/Au}$ ratios (4:25, 8:32, and 14:38). The identified formula of the corresponding species from ESI mass spectra are labeled in (b), where SR denotes *p*-MBA.

DOI: 10.1021/jacs.8b05689
J. Am. Chem. Soc. 2018, 140, 11370–11377

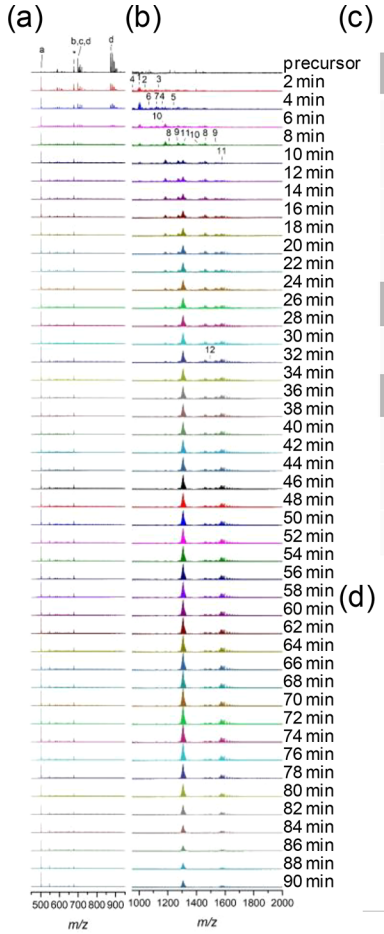

(c)

No.	0 e⁻ Complexes	No.	6 e⁻ NCs
a	$[Au(SR)_2]^-$	5	$Au_{20}(SR)_{14}$
b	$Au_4(SR)_4$	6	$Au_{21}(SR)_{15}$
c	$Au_6(SR)_6$	7	$[Au_{21}(SR)_{16}]^-$
d	$Au_{10}(SR)_{10}$	8	$Au_{23}(SR)_{17}$
No.	2 e⁻ NCs	9	$Au_{24}(SR)_{18}$
1	$Au_{15}(SR)_{13}$	No.	8 e⁻ NCs
No.	4 e⁻ NCs	10	$[Au_{23}(SR)_{16}]^-$
2	$[Au_{16}(SR)_{13}]^-$	11	$[Au_{25}(SR)_{18}]^-$
3	$[Au_{17}(SR)_{14}]^-$	No.	10 e⁻ NCs
4	$Au_{18}(SR)_{14}$	12	$[Au_{29}(SR)_{20}]^-$

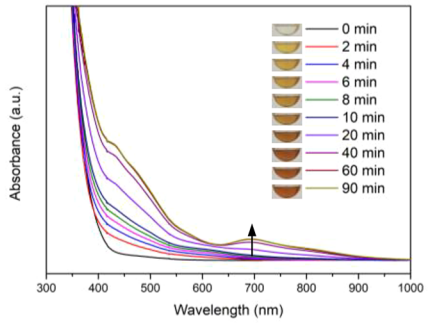

Figure 5. Time-evolution ESI mass spectra (from precursors to the reaction mixture at 90 min after $NaBH_4$ addition) of (a) Au(I)-thiolate complexes and (b) Au NC species in the synthesis of Au NCs using $R_{e/Au}$ = 8:32. (c) Formula of the identified Au(I)-thiolate complexes and Au NC species from ESI mass spectra (SR denotes *p*-MBA). (d) Time evolution UV−vis absorption spectra (from precursors to the reaction mixture at 90 min after $NaBH_4$ addition) of the reaction solution with digital photos (inset).

3^- and 2^- charges, respectively, could be found in the m/z range between 1500 and 4500. By contrast, an additional set of peaks at m/z = 2799 (carrying one negative charge), which were attributed to a Au(I)-thiolate complex, $Au_8(SR)_8$, appeared in the mass spectrum of $R_{e/Au}$ = 4:25 (blue line), indicating these Au(I)-thiolate complexes were not completely reduced by the electrons under this $R_{e/Au}$ ratio (this species was likely formed from partial reduction of $Au_{10}(SR)_{10}$). On the other hand, this set of peaks cannot be spotted when increasing the $R_{e/Au}$ ratio to 14:34. Instead, two additional sets of peaks at m/z = 3718 and 4215 (both carrying three negative charges) emerged in the spectrum. The isotope pattern analysis reveals that these two sets of peaks were attributed to $Au_{38}(SR)_{24}$ and $[Au_{44}(SR)_{26}]^{2-}$ (isotope pattern analysis in Figure S8, Supporting Information). The n^* of the two Au NC species were 14 and 20, respectively, which are larger than that of $[Au_{25}(SR)_{18}]^-$. It is worth noting that these two NC species can be synthesized from $[Au_{25}(SR)_{18}]^-$ using a seed-mediated growth approach.[18] PAGE analysis of the as-synthesized Au NCs agrees well with the ESI-MS results on the composition. As shown in Figure 4c, only one band can be observed when $R_{e/Au}$ = 4:25 and 8:32, while multiple bands exist in the gel for $R_{e/Au}$ = 14:38.

Our experimental results indicate that when $R_{e/Au}$ = 8:32, it is the stoichiometric synthesis for $[Au_{25}(SR)_{18}]^-$. By providing 8 e^- to every 32 Au atoms, the electrons were neither deficient (leaving Au(I)-thiolate complexes (except $[Au(SR)_2]^-$) unreduced, which is the case for $R_{e/Au}$ = 4:25) nor in excess (resulting in Au NCs with larger n^*, which is the case for $R_{e/Au}$ = 8:25 and 14:38). In addition, the yield of Au NCs synthesized when $R_{e/Au}$ = 8:32 was 79 ± 1% (on a Au atoms basis) as measured by ICP-OES. Its proximity to the theoretical yield (78%) according to eq 2 further confirms the stoichiometry of the proposed reduction reaction. The stoichiometric synthesis is applicable in the synthesis of $[Au_{25}(SR)_{18}]^-$ protected by other ligands, such as *m*-mercaptobenzoic acid, thiolsalicylic acid, and glutathione, as shown by their UV−vis absorption spectra in Figure S9 (Supporting Information). In principle, the stoichiometric synthesis of $Au_{38}(SR)_{24}$ could also be conducted when considering $[Au(SR)_2]^-$ as a byproduct. However, $Au_{38}(SR)_{24}$ is between two stable sizes of *p*-MBA-protected Au NCs ($[Au_{25}(SR)_{18}]^-$ and $[Au_{44}(SR)_{26}]^{2-}$, which might have similar stabilities), making it difficult to obtain monodispersed $Au_{38}(SR)_{24}$. Nevertheless, the coexistence of $[Au_{25}(SR)_{18}]^-$ (with smaller n^*) and $[Au_{44}(SR)_{26}]^{2-}$ (with larger n^*) is in good accordance with the stoichiometry we have determined for this particular reaction.

To understand the thermodynamic driving force to form $[Au(SR)_2]^-$ instead of free thiolates as byproduct, we computed the reaction energy difference between eq 2 and eq 1, by using $[Au(SR)]_4$ (i.e., x = 4) as a model Au(I)-thiolate

DOI: 10.1021/jacs.8b05689
J. Am. Chem. Soc. 2018, 140, 11370−11377

complex species. We used the density functional theory (DFT) method with the TPSS functional, the def2-TZVP basis set, and the COSMO implicit solvation model (see Experimental Section for more details). We found that eq 2 is indeed more favorable than eq 1 by 400 kJ/mol, confirming our experimental findings. In other words, formation of $[Au(SR)_2]^-$ rather than free thiolates as a byproduct helps more in driving the formation of $[Au_{25}(SR)_{18}]^-$.

Mechanistic Insights into the Stoichiometric Synthesis of $[Au_{25}(SR)_{18}]^-$. The successful demonstration of stoichiometric synthesis of atomically precise Au NCs opens up a new platform for in-depth investigation into the Au NC growth process. For example, monitoring the intermediates in this $NaBH_4$-mediated reduction-growth process by employing real-time ESI-MS technique becomes easy as the amount of $NaBH_4$ is greatly reduced to the minimum level for the reaction to complete (stoichiometric level). Figure 5a and b show the ESI mass spectra of the reaction solution before (precursors) and after $NaBH_4$ addition, up to 90 min with a time interval of 2 min, for the stoichiometric synthesis of $[Au_{25}(SR)_{18}]^-$. As expected, the product consisted of monodispersed $[Au_{25}(SR)_{18}]^-$, where the only two sets of peaks at 90 min in Figure 5b corresponded to this species (species 11). When we investigated the time-evolution ESI mass spectra, we identified 4 Au(I)-thiolate complexes and 12 Au NC species in total, as listed in Figure 5c (isotope analysis in Figures S10–S21, Supporting Information). More intermediate species were identified compared with the reaction using $R_{e/Au}$ = 8:25, partly because the number of inorganic ions (from reducing agent) was further reduced, most likely due to the reduced number of inorganic ions (from the reducing agent), as well as the relatively slower reaction kinetics, which could further elongate the intermediates' lifetime. We then plotted the ESI-MS peak intensity of these species against reaction time in Figure 6 to better understand the reaction mechanisms.

It can be seen from Figure 6 that the intensity of $[Au(SR)_2]^-$ (species 1) was increased with reaction time, which is consistent with our findings that this species was formed as a byproduct during the reaction. As there was less reducing agent, the reaction kinetics became slower, evidenced from the longer consumption time of Au(I)-thiolate complexes (species b–d). Furthermore, the evolution of Au NC intermediate species provided more information on the growth process of $[Au_{25}(SR)_{18}]^-$. All intermediates identified have even numbered n^* with sequential appearance, suggesting the growth of Au NCs underwent a 2 e^- reduction with a bottom-up growth mechanism using $NaBH_4$ as reducing agent, which is similar to the reported growth mechanism using CO as reducing agent.[10] The Au(I)-thiolate complexes were first reduced by hydride provided by $NaBH_4$ (which is a 2 e^- donor). The reduction led to the formation of 2 e^- intermediates, where $Au_{15}(SR)_{13}$ was the only 2 e^- intermediate found in the time-evolution ESI mass spectra. It was followed by the growth of Au NCs into a mixture with various sizes. These Au NC intermediates have an n^* of 2 e^-, 4 e^-, 6 e^-, 8 e^-, or 10 e^-. Finally, with further reduction or interconversion reactions on the intermediate species, the intermediate species were converted into the thermodynamically stable species, $[Au_{25}(SR)_{18}]^-$. We are able to balance the chemical equations of these reactions in the growth of $[Au_{25}(SR)_{18}]^-$, constructing the reaction mechanism of this $NaBH_4$-mediated growth of atomically precise Au NCs.

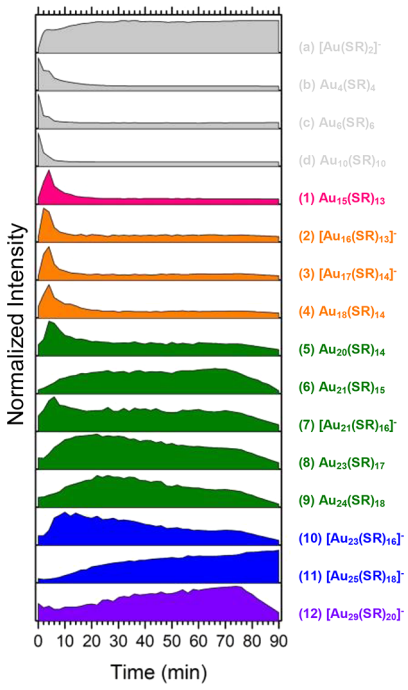

Figure 6. Time-dependent ESI-MS spectral intensity of Au(I)-thiolate complexes and Au NC species in the synthesis of Au NCs using $R_{e/Au}$ = 8:32.

Scheme 1 provides a generalized form of the equations. It can be seen that the reduction reactions were the important source of $[Au(SR)_2]^-$ formation, as in the balanced reduction reactions $[Au(SR)_2]^-$ is on the product side. This is consistent with the experimental findings that the peaks of $[Au(SR)_2]^-$ were rapidly increased after the addition of reducing agent (i.e., first 10 min of reactions). In this stage, the reduction reactions were dominant when the reducing agent was abundant. Despite being from the reduction reactions, $[Au(SR)_2]^-$ was also the byproduct of some interconversion reactions (e.g., metathesis reaction between $[Au_{21}(SR)_{16}]^-$ and $Au_4(SR)_4$ to form $Au_{24}(SR)_{18}$ and $[Au(SR)_2]^-$). Together with the slow reduction reactions in the subsequent stage, the abundance of $[Au(SR)_2]^-$ continuously grew, which again matches with our time-evolution ESI mass spectra. Therefore, from the growth rate of $[Au(SR)_2]^-$, we can also conclude the two-stage growth mechanism of Au NCs in the $NaBH_4$ reduction synthesis: a fast reduction–growth stage followed by a slow size-focusing stage. Time-evolution UV–vis absorption spectra in Figure 5d also confirm the two-stage mechanism, where the characteristic absorption peaks of $[Au_{25}(SR)_{18}]^-$ at 430 and 690 nm only appeared at ~10 min after $NaBH_4$ addition.

Scheme 1. General Balanced (Half) Equations of Reduction Reaction, Addition Reaction, Metathesis Reaction, and Comproportionation Reaction during the Growth Process of Au NCs

Reduction Reaction:

$$[Au_n(SR)_m]^q + [Au(SR)]_x + 2\,e^- = [Au_{n+x-y}(SR)_{m+x-2y}]^{q+y-2} + y\,[Au(SR)_2]^-$$

Addition Reaction:

$$[Au_n(SR)_m]^q + [Au(SR)]_x = [Au_{n+x}(SR)_{m+x}]^q$$

Metathesis Reaction:

$$[Au_n(SR)_m]^q + [Au(SR)]_x = [Au_{n+x-y}(SR)_{m+x-2y}]^{q+y} + y\,[Au(SR)_2]^-$$

Comproportionation Reaction:

$$[Au_{n1}(SR)_{m1}]^q + [Au_{n2}(SR)_{m2}]^q = 2\,[Au_{(n1+n2)/2}(SR)_{(m1+m2)/2}]^q$$

DOI: 10.1021/jacs.8b05689
J. Am. Chem. Soc. 2018, 140, 11370–11377

CONCLUSION

In conclusion, we have successfully demonstrated the stoichiometric synthesis of $[Au_{25}(SR)_{18}]^-$, with the amount of $NaBH_4$ used greatly reduced by ~320 times compared with that used in the conventional synthesis. The stoichiometric $R_{e/Au}$ ratio was found to be 8:32, as an important Au-containing byproduct, $[Au(SR)_2]^-$, was identified. The finding that $[Au(SR)_2]^-$ was the byproduct instead of free thiolates in the synthesis is important, as it advances the understandings on the fate of the Au atoms and thiolate ligands in the growth process. In addition, the stoichiometric synthesis of $[Au_{25}(SR)_{18}]^-$ allows mechanistic exploration of Au NC synthesis with $NaBH_4$ as reducing agent. With the identification of the intermediate species, we have determined the reactions during the reduction and interconversion process, constructing the two-stage 2 e^- reduction−growth mechanism for $[Au_{25}(SR)_{18}]^-$ in the $NaBH_4$ reduction synthesis.

EXPERIMENTAL SECTION

Chemicals. All chemicals were used as purchased without purification. Gold tetrachloride trihydrate ($HAuCl_4{\cdot}3H_2O$), 4-mercaptobenzoic acid (*p*-MBA), sodium borohydride ($NaBH_4$), acetic acid (AcOH), and sodium chloride (NaCl) were purchased from Sigma-Aldrich. Sodium hydroxide (NaOH) was purchased from Merck. Ethanol and dimethylformamide (DMF) were purchased from VWR. Nitrogen gas (N_2) was provided by SOXAL. Ultrapure water (Milli-Q) with a resistivity of 18.2 MΩ·cm (bubbled with N_2 for 2 min to remove dissolved O_2) was used as the solvent for the synthesis.

Synthesis of Gold Nanoclusters. In a typical synthesis of $[Au_{25}(SR)_{18}]^-$ using a stoichiometric $R_{e/Au}$ ratio (8:32), aqueous solutions of *p*-MBA (50 mM in 150 mM NaOH, 0.2 mL) and $HAuCl_4$ (20 mM, 0.25 mL) were added to 4.4 mL of ultrapure water under 500 rpm stirring at room temperature. After 30 min, the pH of the solution was brought to 11.5 by adding 1 M NaOH. After that, a $NaBH_4$ solution (1 mM in 1 mM NaOH, 0.156 mL) was added to the reaction solution under a nitrogen atmosphere with 1000 rpm vigorous stirring. One minute later, the magnetic stirrer was switched off and the reactants were allowed to react without stirring for an additional 89 min. For the synthesis under different $R_{e/Au}$ ratios, the synthesis process was similar to that used in $R_{e/Au}$ = 8:32, except for the addition of a different volume of water (making the total volume of reaction solution 5 mL) and a 1 mM $NaBH_4$ solution.

Characterization of Gold Nanoclusters. Sample pretreatments were required before some characterizations. Before characterizing the products by ESI-MS, the Au NC solution (0.2 mL) was first precipitated by adding 20 μL of a 2.5 M NaCl solution and 1.3 mL of ethanol. The mixture was then centrifuged at 10 000 rpm for 6 min at room temperature. The resulting pellet was washed by DMF (1 mL) and centrifuged at 10 000 rpm for 3 min at room temperature. The pellet was then dissolved in 50 μL of AcOH and 450 μL of DMF for ESI-MS measurement. Before characterizing the products by PAGE and ICP-AES, the samples were purified by ultrafiltration using a filter with a molecular weight cutoff (MWCO) of 5000 Da. Sample pretreatment was not required for real-time ESI-MS and UV−vis absorption spectra characterizations.

ESI mass spectra were measured on a Bruker MicroTOF-Q ESI time-of-flight system operating in negative ion mode. The sample injection rate was set as 3 L·min^{-1} by the syringe pump. Other ESI-MS parameters are nebulizer 1.5 bar, capillary voltage 4 kV, dry gas 4 L·min^{-1} at 120 °C, and m/z range 100−3000. For real-time ESI-MS measurement, a sufficient amount of reaction solution (about 0.4 mL) was taken out by a syringe after 1 min of mixing. The syringe was then put on a syringe pump, which is connected to the ESI-MS. UV−vis absorption spectra were measured on a Shimadzu UV-1800 spectrometer. For real-time UV−vis absorption measurement, a sufficient amount of reaction solution (about 1 mL) was taken out into a quartz cuvette after 1 min of mixing. Native PAGE was carried out on a Bio-Rad Mini-PROTEAN Tetra Cell system. Stacking and resolving gels were prepared from 4 and 30 wt % acrylamide monomers, respectively. A gel slab of 1.0 × 83 × 73 mm in dimension was used. Sample solutions (10 μL of Au NCs with 6 mM Au in 8 vol % glycerol) were loaded into the wells of the stacking gel. The electrophoresis was allowed to run for about 4 h at a constant voltage of 150 V at 4 °C. Yields of Au NCs were measured on a PerkinElmer Optima 5300DV inductively coupled plasma atomic emission spectrometer.

Computation Details. DFT calculations were performed using the TPSS form[19] of the meta-GGA (generalized gradient approximation)[20] functional for the electron exchange and correlation energy, as implemented in Turbomole v6.5.[21] Def2-TZVP basis sets were used for the main group elements,[22] and effective core potentials with 19 valence electrons were used for Au.[23] The energy of the species in solvation was calculated using the conductor-like screening model (COSMO) in Turbomole.[24]

ASSOCIATED CONTENT

Supporting Information

The Supporting Information is available free of charge on the ACS Publications website at DOI: 10.1021/jacs.8b05689.

Additional information (PDF)

AUTHOR INFORMATION

Corresponding Author

*chexiej@nus.edu.sg

ORCID

Tiankai Chen: 0000-0003-0730-3373
Qiaofeng Yao: 0000-0002-5129-9343
Zhentao Luo: 0000-0002-3074-046X
De-en Jiang: 0000-0001-5167-0731
Jianping Xie: 0000-0002-3254-5799

Notes

The authors declare no competing financial interest.

ACKNOWLEDGMENTS

We acknowledge the financial support from the Ministry of Education, Singapore, Academic Research Grant R-279-000-481-112. V.F. and D.-e.J. were supported by the Division of Chemical Sciences, Geosciences and Biosciences, Office of Basic Energy Sciences, U.S. Department of Energy. T.C. acknowledges National University of Singapore for a research scholarship.

REFERENCES

(1) (a) Bokhoven, C.; Gorgels, M. J.; Mars, P. *Trans. Faraday Soc.* **1959**, *55*, 315. (b) Flagan, R. C.; Seinfeld, J. H. *Fundamentals of Air Pollution Engineering*; Courier Corporation, 2012.

(2) Rossberg, M.; Lendle, W.; Pfleiderer, G.; Tögel, A.; Dreher, E.-L.; Langer, E.; Rassaerts, H.; Kleinschmidt, P.; Strack, H.; Cook, R.; Beck, U.; Lipper, K.-A.; Torkelson, T. R.; Löser, E.; Beutel, K. K.; Mann, T. In *Ullmann's Encyclopedia of Industrial Chemistry*; Wiley-VCH Verlag GmbH & Co. KGaA: 2000.

(3) Ishiyama, T.; Nobuta, Y.; Hartwig, J. F.; Miyaura, N. *Chem. Commun.* **2003**, 2924.

(4) Brust, M.; Walker, M.; Bethell, D.; Schiffrin, D. J.; Whyman, R. *J. Chem. Soc., Chem. Commun.* **1994**, *801*, 801.

(5) (a) Li, Y.; Zaluzhna, O.; Xu, B. L.; Gao, Y. A.; Modest, J. M.; Tong, Y. J. *J. Am. Chem. Soc.* **2011**, *133*, 2092. (b) Frenkel, A. I.; Nemzer, S.; Pister, I.; Soussan, L.; Harris, T.; Sun, Y.; Rafailovich, M. H. *J. Chem. Phys.* **2005**, *123*, 184701.

(6) Zhao, P. X.; Feng, X. W.; Huang, D. S.; Yang, G. Y.; Astruc, D. *Coord. Chem. Rev.* **2015**, *287*, 114.

DOI: 10.1021/jacs.8b05689
J. Am. Chem. Soc. 2018, 140, 11370−11377

(7) (a) Qian, H. F.; Zhu, M. Z.; Wu, Z. K.; Jin, R. C. *Acc. Chem. Res.* **2012**, *45*, 1470. (b) Chakraborty, I.; Pradeep, T. *Chem. Rev.* **2017**, *117*, 8208. (c) Knoppe, S.; Burgi, T. *Acc. Chem. Res.* **2014**, *47*, 1318. (d) Goswami, N.; Yao, Q. F.; Chen, T. K.; Xie, J. P. *Coord. Chem. Rev.* **2016**, *329*, 1.
(8) Jiang, D. E. *Nanoscale* **2013**, *5*, 7149.
(9) Hakkinen, H. *Chem. Soc. Rev.* **2008**, *37*, 1847.
(10) Luo, Z. T.; Nachammai, V.; Zhang, B.; Yan, N.; Leong, D. T.; Jiang, D. E.; Xie, J. P. *J. Am. Chem. Soc.* **2014**, *136*, 10577.
(11) Chen, T. K.; Luo, Z. T.; Yao, Q. F.; Yeo, A. X. H.; Xie, J. P. *Chem. Commun.* **2016**, *52*, 9522.
(12) (a) Chatenet, M.; Micoud, F.; Roche, I.; Chainet, E.; Vondrak, J. *Electrochim. Acta* **2006**, *51*, 5452. (b) Lo, C. T. F.; Karan, K.; Davis, B. R. *Ind. Eng. Chem. Res.* **2007**, *46*, 5478.
(13) (a) Yuan, X.; Zhang, B.; Luo, Z. T.; Yao, Q. F.; Leong, D. T.; Yan, N.; Xie, J. P. *Angew. Chem., Int. Ed.* **2014**, *53*, 4623. (b) Chen, T. K.; Yao, Q. F.; Yuan, X.; Nasaruddin, R. R.; Xie, J. P. *J. Phys. Chem. C* **2017**, *121*, 10743.
(14) Black, D. M.; Alvarez, M. M.; Yan, F. Z.; Griffith, W. P.; Plascencia-Villa, G.; Bach, S. B. H.; Whetten, R. L. *J. Phys. Chem. C* **2017**, *121*, 10851.
(15) Iacobucci, C.; Reale, S.; De Angelis, F. *Angew. Chem., Int. Ed.* **2016**, *55*, 2980.
(16) (a) Dharmaratne, A. C.; Krick, T.; Dass, A. *J. Am. Chem. Soc.* **2009**, *131*, 13604. (b) Qian, H. F.; Zhu, Y.; Jin, R. C. *ACS Nano* **2009**, *3*, 3795.
(17) (a) Barngrover, B. M.; Aikens, C. M. *J. Phys. Chem. Lett.* **2011**, *2*, 990. (b) Barngrover, B. M.; Aikens, C. M. *J. Am. Chem. Soc.* **2012**, *134*, 12590.
(18) Yao, Q. F.; Yuan, X.; Fung, V.; Yu, Y.; Leong, D. T.; Jiang, D. E.; Xie, J. P. *Nat. Commun.* **2017**, *8*, 927.
(19) Tao, J. M.; Perdew, J. P.; Staroverov, V. N.; Scuseria, G. E. *Phys. Rev. Lett.* **2003**, *91*, 146401.
(20) Perdew, J. P.; Burke, K.; Ernzerhof, M. *Phys. Rev. Lett.* **1996**, *77*, 3865.
(21) Ahlrichs, R.; Bar, M.; Haser, M.; Horn, H.; Kolmel, C. *Chem. Phys. Lett.* **1989**, *162*, 165.
(22) (a) Weigend, F.; Haser, M.; Patzelt, H.; Ahlrichs, R. *Chem. Phys. Lett.* **1998**, *294*, 143. (b) Weigend, F.; Ahlrichs, R. *Phys. Chem. Chem. Phys.* **2005**, *7*, 3297.
(23) Andrae, D.; Haussermann, U.; Dolg, M.; Stoll, H.; Preuss, H. *Theor. Chim. Acta.* **1990**, *77*, 123.
(24) Klamt, A.; Schuurmann, G. *J. Chem. Soc., Perkin Trans. 2* **1993**, *2*, 799.

DOI: 10.1021/jacs.8b05689
J. Am. Chem. Soc. 2018, 140, 11370−11377